

01 Aug 1998

Time History Extrapolation for FDTD Modeling of Shielding Enclosure Designs and EMI Antenna Geometries

Xiao Luo

Min Li

James L. Drewniak

Missouri University of Science and Technology, drewniak@mst.edu

Follow this and additional works at: https://scholarsmine.mst.edu/ele_comeng_facwork

 Part of the [Electrical and Computer Engineering Commons](#)

Recommended Citation

X. Luo et al., "Time History Extrapolation for FDTD Modeling of Shielding Enclosure Designs and EMI Antenna Geometries," *Proceedings of the IEEE International Symposium on Electromagnetic Compatibility (1998, Denver, CO)*, vol. 2, pp. 1172-1177, Institute of Electrical and Electronics Engineers (IEEE), Aug 1998.

The definitive version is available at <https://doi.org/10.1109/ISEMC.1998.750375>

This Article - Conference proceedings is brought to you for free and open access by Scholars' Mine. It has been accepted for inclusion in Electrical and Computer Engineering Faculty Research & Creative Works by an authorized administrator of Scholars' Mine. This work is protected by U. S. Copyright Law. Unauthorized use including reproduction for redistribution requires the permission of the copyright holder. For more information, please contact scholarsmine@mst.edu.

Time History Extrapolation for FDTD Modeling of Shielding Enclosure Designs and EMI Antenna Geometries

X. Luo, M. Li and J. L. Drewniak
Electromagnetic Compatibility Laboratory
Department of Electrical Engineering
University of Missouri at Rolla
Rolla, MO 65409

Abstract: The GPOF (Generalized Pencil-Of-Function) method was used to extrapolate the time response from FDTD simulations of EMI problems by approximating the time history as a sum of complex exponentials. This method can significantly shorten the FDTD program execution time. However, various difficulties can arise from parameterization during data-processing. The GPOF is applied to, and studied for, two relevant EMI problems, enclosure design and EMI antenna modeling. The merits of GPOF in modeling shielding enclosures and EMI antennas is evaluated through several examples.

I. INTRODUCTION

A significant advantage of the FDTD method in simulating EMI problems is that a wide frequency range can be computed simultaneously. Usually, a field value, current or voltage on a structure or scattered field at a point in space that result from an exciting pulse are recorded in time. The total computation duration depends on the time it takes the field to reach steady state or achieve a late-time history. If the problem space is a high- or moderate- Q resonant geometry, where the field dissipation is slow, the number of time steps required for a response sequence to produce a complete frequency band without distortion or loss of information will be large.

Time-domain solutions of an EMI problem (E or H field, voltage, current) using FDTD modeling are ultimately utilized in computing physical parameters such as impedance and S -parameters, which are defined in frequency domain. Typically, the time history from the FDTD data are transformed into the frequency domain with an FFT. However, for long time histories the memory required, and storage and processing can be prohibitive on top of a long FDTD computation time. Other techniques have been developed for extrapolating a time-history from only a short segment of the original FDTD time record. Many of these approaches, for example, MUSIC [1], SI [2], Prony [3] and Pencil of Function (POF) [4] are well-known as signal-processing techniques that originally found their useful application in target identification [5], spectral estimation, and digital filtering [6]. Recently, Prony's method and the Pencil of Function have been recognized as two powerful techniques to estimate parameters of exponentially damped sinusoidal signals contaminated by noise. The Generalized Pencil Of Function (GPOF) is a refined version of POF [8].

Prony's method has been found accurate for extracting poles and residues from given equally spaced transient data. However, it is notorious for its extreme sensitivity to noise [9] [10]. Approaches have been investigated to minimize the sensitivity in

Prony's method through optimizing the sampling scheme [11]. The noise sensitivity of the GPOF method has also been studied based on a simplified sequence consisting of computer-generated numerical samples of fewer than three modes and typical Gaussian white noise [8]. Prony's method has been combined with FDTD to analyze microwave integrate circuits [3]. GPOF has recently been used for extracting poles from limited MOM data to give a stable long time history from the original unstable solution [12]. This application indicates that GPOF works fairly well for a data sequence with fewer than ten modes.

Prony's method employs a polynomial approach and is much older than the the Generalized Pencil Of Function. The GPOF method uses a one-step process to solve a nonlinear equation through the solution of a generalized eigenvalue problem, as opposed to two steps, as with Prony and POF. Further, both Prony's method and GPOF can be implemented in terms of matrix equation, and GPOF results in general much better conditioned matrix.

This paper presents a study of time-history extrapolation using GPOF for EMI antenna and enclosure geometries. The GPOF method is reviewed within the scope of its application to FDTD. Guidelines for choosing the parameters are discussed based on a real-time FDTD history. Finally, numerical examples are presented to show the effectiveness of GPOF in modeling geometries relevant to EMI applications.

II. GPOF OVERVIEW

A brief review of the GPOF method is presented here for the purpose of defining the parameters that are discussed in the numerical examples. A detailed mathematical development can be found in references [7] and [8]. Briefly, the problem to be solved is: given a time response $I(t)$ from an FDTD simulation (current, voltage, or field), it is assumed that $I(t)$ can be expressed as

$$I(t) = \sum_{i=1}^M A_i Z_i \quad (1)$$

$$Z_i = e^{s_i \delta t} \quad (2)$$

with parameters

M : number of poles, or modes
 A_i : residues or complex amplitude
 $S_i = \alpha_i + j\omega_i$: poles
 α_i : damping factors
 ω_i : angular frequencies

δt : FDTD sampling interval

the best estimated of M , A_i and S_i is desired. The most difficult part of this problem is finding the Z_i . After the Z_i are determined, A_i is found by solving a matrix equation [8].

Suppose $x(j)$, $j = 1, 2, 3, \dots, P$ is a sequence of data from an FDTD simulation with up to P time steps. A sampling window of size $N < P$ steps is chosen, and a time decimation factor of d is used the beginning at the $j = ni$ time step. The purpose of the sampling window will be demonstrated later in this section. The new sampled sequence is

$$y_k = x(ni + k \times d), k = 0, 2, \dots, N-1, \quad (3)$$

which consists of N points covering the original sequence from $x(ni)$ to $x(ni + k \times N)$. The reduced segment over the window N is

$$y_k = \sum_{j=1}^M A_j Z_j \quad (4)$$

A data matrix $[Y]$ based on input vector y_k is defined as

$$[Y] = \begin{bmatrix} y_0 & y_1 & \cdots & y_L \\ y_1 & y_2 & \cdots & y_{L+1} \\ \vdots & \vdots & \ddots & \vdots \\ y_{N-L-1} & y_{N-L} & \cdots & y_{N-1} \end{bmatrix}_{(N-L) \times (L+1)} \quad (5)$$

and two further additional matrices $[Y_1]$ and $[Y_2]$ defined simply from $[Y]$ by deleting the first column, and last column, respectively, are

$$[Y_1] = \begin{bmatrix} y_1 & y_2 & \cdots & y_L \\ y_2 & y_3 & \cdots & y_L \\ \vdots & \vdots & \ddots & \vdots \\ y_{N-L} & y_{N-L+1} & \cdots & y_{N-1} \end{bmatrix}_{(N-L) \times (L)} \quad (6)$$

$$[Y_2] = \begin{bmatrix} y_0 & y_1 & \cdots & y_{L-1} \\ y_1 & y_2 & \cdots & y_L \\ \vdots & \vdots & \ddots & \vdots \\ y_{N-L-1} & y_{N-L} & \cdots & y_{N-2} \end{bmatrix}_{(N-L) \times (L)} \quad (7)$$

where L is an initial guess for M , $M \leq N$, and $M \leq N - L$. L must be less than N in all matrices $[Y]$, $[Y_1]$ and $[Y_2]$. In an ideal case, when the data matrix $[Y]$ contains signals that can be expanded in M modes, there will be only M independent vectors associated with the matrix $[Y]$, the remaining $L - M$ vectors of the matrix $[Y]$ will be dependent. It can be shown that if y_k satisfies the Eq. (4), then Z_i can be solved as an eigenvalue problem [8], namely

$$[Y_1]^+ [Y_2] - Z[I] = 0 \quad (8)$$

Eq.(8) can be solved only if the rank of the matrix M , is known. In the above discussion, since the matrix $[Y]$ contains all information in segment $x(ni) \dots x(ni + N \times dn)$, it has

been assumed that the same Eq.(4) will fit the late history $x(ni + N \times dn) \dots x(P)$, when almost all components die down. But this is an approximation because the early time history contains components, or "noise" that will vanish in the late time history. Therefore, information about the speed at which these components are damped, as well as how small damped magnitude should be, must be reflected in the data matrices $[Y_1]$ and $[Y_2]$, so that finally it can be quantified in the damping factors α_i , the real part of S_i . Singular Value Decomposition (SVD) is utilized to compensate for the "noise" in the early time history and determine M . SVD of the matrix $[Y]$ can be represented by [13]

$$[U]^H [Y] [V] = \lambda \quad (9)$$

where "H" denotes the conjugate transpose of a matrix. $[U]$ and $[V]$ are unitary matrices that composed of eigenvectors of $[Y][Y]^H$ and $[Y]^H[Y]$. The λ_i , $i = 1, 2, \dots, L$ are singular values of $[Y]$ in decreasing order. The range of λ physically represents the "noise" level relative to the signal level, or, mathematically, how close the noisy matrix is to singular. The closer $[Y]$ is to singular, the more difficult it is to adequately determine $[Y]^{-1}$.

The ratios of the singular values over the maximum singular value are calculated

$$\frac{\lambda_i}{\lambda_{max}} \geq \sigma, i = 2, 3, \dots, M-1, M \quad (10)$$

where σ and M characterize the distribution of singular values. If the ratio below some specified σ is too small, then the $L - M$ small singular values correspond to noise are not used to estimate the late time history. As a result, only the M singular values sufficiently large to satisfy Eq.(10) are used. The final step is to reconstruct the matrix Y_1 and Y_2 from the M large singular values, substitute in Eq.(8) and solve for the Z_i , $i = 1, 2, \dots, M-1, M$.

III. A STUDY OF INPUT PARAMETERS

There are two issues that must be addressed before applying GPOF to an FDTD time history. First is the selection of the segment of the FDTD time history to be used for the estimation. The segment should cover a significant fraction of an FDTD time history exhibiting its damping and oscillating nature. The other requirement is that the original FDTD record must undergo some decimation. To meet the FDTD stability condition [14], the FDTD sampling is more dense than needed to apply the GPOF method. In general, a sampling window with a decimation factor is put on the original FDTD early time history to give the input data for the GPOF extrapolation procedure.

The GPOF method is evaluated here based on accuracy and stability. The newly-constructed time history based on the GPOF estimation procedure is desired to be the same as the original FDTD time sequence. Then, in frequency domain, their FFT spectrum should also be the same. Comparison can be done on a point-by-point basis of the old and new data. Another way of assessing the accuracy is to introduce a signal to noise ratio, which is defined here as

$$SNR(dB) = 10 \log_{10} \frac{\sum (new - old)^2}{\sum (old)^2} \quad (11)$$

whereas “new” denotes the newly constructed time history by GPOF, and “old” denotes the original FDTD time history. Summation starts from $x(n_i)$ to $x(P)$. The SNR is used herein to compare the accuracy of the GPOF method applied to the FDTD time history resulting from modeling different EMI geometries. The SNR is a more global check of time-domain curve fitting. Stability is ensured for the α_i all negative. A solution with any positive α is usually discarded independent of the SNR. Further, solutions with poor SNR, such as < 10 dB are also discarded.

The algorithm was implemented with input parameters of the width and location of the sampling window, L the size of the data matrix and the criteria σ . While the above process to achieve accuracy and stability appears straightforward, in practice, choosing the input parameters in order to obtain a good solution can be arduous. A parametric study of GPOF for EMI applications is discussed below.

The time history for the current at the feed point of a driven shielding enclosure geometry is used for conducting the parametric study. This sequence is essential in computing delivered power to a real cavity, and is supported by experimental results [15]. In Table I, n_i is the initial sampling time step used in GPOF, P_s is the maximum current value in the sampling sequence $y(k)$, and P_m is the peak value of the original time history. The ratio is indicative of the position of the sampling window relative to the complete time history, and also the degree of damping. The decimation factor d indicates the sampling interval of the original FDTD time sequence. The value of d and σ are kept constant for all the tabulated results. In each case, poles and residues are estimated. If any damping factors are positive, the solution is labeled as unstable. The SNR is calculated from $x(n_i)$ to the latest time history $x(P)$. M is the number of terms after noise deleting, as represented in Eq.(1). L is the estimation of number of terms before noise-deleting and was 80 in all cases. When the sampling window is moved backward from late time history to early time history, M varies randomly within the range of 14 – 24. When $n_i > 2300$ steps and $P_s/P_m < 0.5$, a stable solution with good accuracy results. The accuracy of the solution in terms of an acceptable SNR is assessed from a point by point comparison of the time domain results for the original FDTD sequence and the GPOF extrapolated sequence. If the sampling window is located too early in the time sequence, so that $n_i < 2300$ and $P_s/P_m > 0.5$, the extrapolation is more likely to be unstable. Even for the few stable solutions within this region, the accuracy is usually poor. The sampling window ($N = 250$, $d = 10$) is unsuitable for $n_i < 2300$ and $P_s/P_m > 0.5$.

The condition number of the matrix $[Y]$ is the ratio of the largest singular value and the smallest singular value

$$cond = \frac{\lambda_{max}}{\lambda_{min}} \quad (12)$$

The tolerance of the matrix $[Y]$ is defined as the inverse of the condition number

$$\tau = \frac{1}{cond} \quad (13)$$

TABLE I
The Influence of Sampling Time Start on Stability and Accuracy ($\sigma = 3.0e - 5$, $d = 10$ steps, $N = 250$ points)

Location n_i	P_s/P_m	M	Stability	SNR (dB)
7000	0.1048	19	yes	24.9
6000	0.1447	17	yes	25.0
5000	0.1447	24	yes	24.8
4000	0.2503	17	yes	25.2
3700	0.2503	20	yes	25.7
3500	0.2524	19	yes	25.4
3300	0.3498	19	yes	26.4
3000	0.3498	17	yes	26.9
2900	0.3498	20	yes	27.0
2700	0.4044	14	yes	26.5
2600	0.488	19	yes	26.7
2500	0.5672	17	yes	26.6
2400	0.6032	17	yes	28
2300	0.6032	17	no	27.8
2200	0.6032	12	yes	29.1
2000	0.6032	8	yes	-0.8
1000	0.9243	19	no	-399

Figure 1 shows the tolerance of the matrix $[Y]$ as a function of the decimation factor d when the sampling window starts at $n_i = 1000$. When $d = 1$, which means the FDTD simulation data is used directly without any sampling, the condition number is a maximum 2×10^8 and the tolerance is the minimum. This makes solving Eq.(4) for poles most difficult. τ increases rapidly as sampling interval increases to 10. The larger the τ , the easier to solve the equation. τ slow down after $d > 20$. But τ did not go up steady, especially when d changes slightly within 2 – 5 steps.

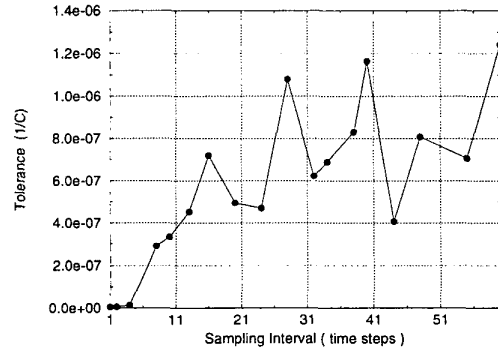


Figure 1. Tolerance of the matrix $[Y]$ as a function of the decimation factor d ($N = 300$, $n_i = 1000$, $L = 0.45 \times N$)

M will be affected by d in a fashion similar to τ due to the inherent connection between σ and $cond$. A suitable value of d for all cases studied falls in the range of 11 – 24, during which a large value of τ reached. A larger d may not necessarily improve the estimation. For example, at $d = 43$, $\tau = 4.0 \times 10^{-7}$, even

lower than when $d = 20$. Moreover, we'll need more early time history for a longer sampling window than a shorter one.

The above discussion illustrates that different sampling window result in a different condition number on the same FDTD time history. In general, the solution for the poles Z_i and M can be quite sensitive to small variations in the sampling window or its location in the early time history. However there does exist a range of n_i for which a stable and accurate solution for this particular enclosure problem is expected. In general, the sampling window should be put in the position so that the ratio $P_s/P_m < 0.5$. The decimation factor d should be in the range of 11-24 to achieve a well-conditioned matrix and a moderate window size.

The value of L limits the number of columns in $[Y]$. Different values of L from $N/2$ to $N/3$ was used and the resulting M was estimated. The stability and accuracy while varying L was investigated. The results in Table II indicated that if the ratio of L/N is close to 0.5, an unstable solution can result. A stable solution resulted for $L/N < 0.45$. The value of M , may, in general, be different for a number of stable solution, depending on the initial choice of L .

TABLE II
The Influence of the Initial Number of Poles (L) on Stability
($N = 200$, $\sigma = 3.0e - 5$, $d = 10$ steps, $n_i = 2800$)

Initial No. of Terms (L)	Actual No. of Terms	Stability
99	18	no
98	20	no
97	20	no
96	19	no
95	20	no
93	21	no
92	22	yes
91	21	yes
90	21	yes
89	22	yes
88	17	yes
85	13	yes
80	20	yes

TABLE III
Effect of σ on accuracy and stability ($N = 200$, $d = 10$ steps,
 $L = 80$, $n_i = 4000$)

σ	Actual No. of Terms (M)	Stability	SNR(dB)
1×10^{-6}	80	no	NA
5×10^{-6}	61	no	NA
8×10^{-6}	50	no	NA
1×10^{-5}	46	no	NA
3×10^{-5}	26	yes	24.5
5×10^{-5}	15	yes	24
8×10^{-5}	11	yes	23
1×10^{-4}	7	yes	17
5×10^{-4}	7	yes	17
8×10^{-4}	7	yes	17
5×10^{-3}	7	yes	17

The effect of σ was also investigated and the results are tabulated in Table III. A σ that is too large will result in a poor SNR, while σ too small will lead to instability. Choosing a proper σ , in this particular example within the order of magnitude of 10^{-5} , is a delicate balance between stability and accuracy. Moreover, a suitable value of σ can vary by 1-2 orders of magnitude for different n_i or d .

IV. APPLICATION OF GPOF

Application of the GPOF method to FDTD time histories from numerical EMI modeling was the focus of this study. In particular, two distinct choices of problems, PCB EMI antenna modeling in open regions, and shielding enclosure geometries are of concern.

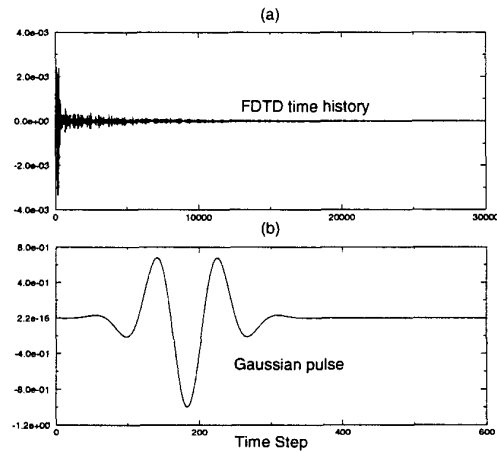


Figure 2. (a) A typical FDTD time response from EMI geometries, and, (b) the Gaussian excitation pulse.

A typical slowly-dissipating time response consisting of a short excitation interval and a long dissipating interval of more than 20,000 steps is shown in Figure 2a. A sinusoidally - modulated Gaussian pulse shown in Figure 2b was used as the excitation voltage source in all examples [15]. An FFT was employed to obtain the frequency-domain response.

Figure 3 shows two relevant EMI structures from which the FDTD simulation data were obtained and time extrapolated with GPOF. Swept frequency measurements have also been made for these structures to compare with the FDTD simulations and GPOF result.

The time- and frequency-domain current at the feed point of a PCB-type dipole antenna geometry illustrated in Figure 3b computed over 5000 FDTD time steps is shown in Figure 4. The current sequence was utilized in computing the input impedance. The input impedance of the EMI antenna geometry is needed for use with source models in order to estimate the common-mode current on the cable and the resulting radiated EMI. For example, modeling coupling of high-speed digital signal to I/O lines requires the EMI antenna input impedance [16].

Sampling for the GPOF extrapolation of 100 data points began at the 100th time step with a decimation factor of 5. The loca-

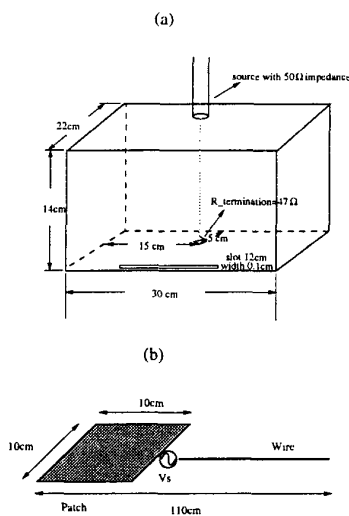


Figure 3. EMI geometries utilized for FDTD simulation, (a) shielding enclosure, and, (b) PCB-type dipole antenna.

tion of the window is chosen so that $P_s/P_m < 0.5$. The decimation factor d was chosen smaller than 10 simply because given an extrapolation as good as $d=11$, but with a much smaller window size. As a result, only the first 600 time steps are required for implementing the GPOF extrapolation. The criteria for singular value elimination, σ , in the GPOF method was 8×10^{-3} , and L the data matrix size was 40. The resulting number of exponentials in the expansion Sampling Eq.(4) was $M=8$. The stable solution had a signal-to-noise ratio (SNR) of 80 dB within the reconstruction region, which shows a high accuracy of GPOF extrapolation for this problem. A comparison of the original FDTD and the GPOF extrapolated data in both the time- and frequency-domain is shown in Figure 3. GPOF saves 70% in computation time while maintaining very high accuracy. The time sequence dissipates relatively quickly making it possible to choose parameters more liberally than those for the enclosure data of Table I.

FDTD and GPOF results for the current at the feed point of a shielding enclosure geometry are shown in Figure 5. The current was recorded for 20,000 FDTD time steps. Sampling for the GPOF extrapolation began at time step $n=150$ and proceeded at intervals of 15 steps for 400 data points of input. The σ was 8×10^{-3} , and L the size of data matrix was 160. After computation of the GPOF algorithm, the number of exponential terms was 42. Guidelines suggested by Table I and Figure 1 are followed for choosing input parameters. However, the GPOF solution was obtained by carefully adjusting the σ and the sampling window. For example, five values of σ were tried between 10^{-5} and 10^{-2} before a suitable value was found. N was increased to capture the slowly damped features characteristic of a nearly closed region problem. The decimation must adequately represent the oscillating sequence, as well as to accommodate a better conditioned matrix. More than five

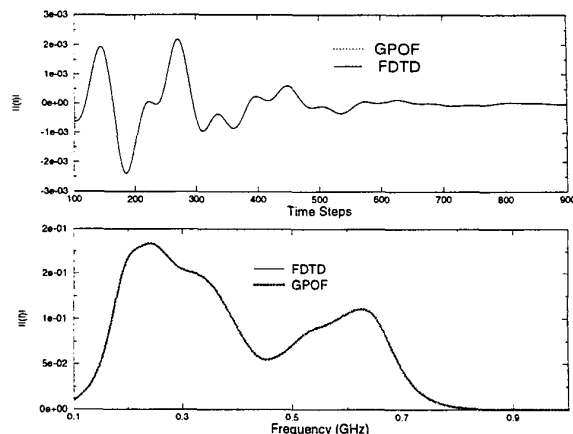


Figure 4. A comparison of FDTD and GPOF results from an EMI antenna geometry in the time domain (upper), and the frequency domain (lower).

different combinations of σ and sampling window were explored until a stable solution with a moderate accuracy of 28 dB (SNR) was achieved. Figure 5 illustrates both the time- and frequency-domain comparison of FDTD and GPOF results. There is a slight magnitude discrepancy in the time response that yields a small deviation at the magnitude of the high-Q resonance in the frequency spectrum. The latter is a result of the resonant cavity geometry. However, GPOF is still beneficial for this problem considering 20,000 FDTD steps were reduced to 6150 time steps using GPOF with acceptable accuracy.

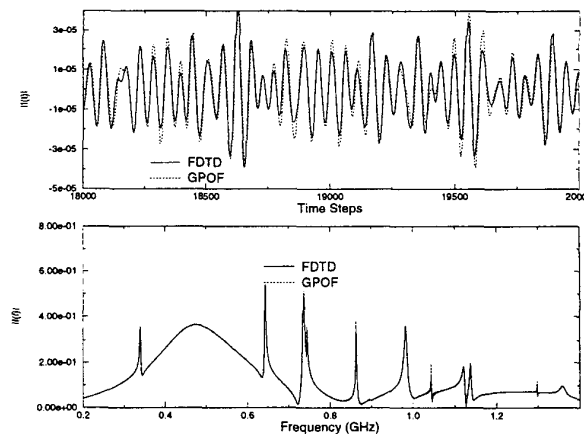


Figure 5. The comparison between FDTD and GPOF constructed current response from shielding enclosure geometry in (Upper) time domain and (Bottom) frequency domain.

In another similar cavity structure, the time- and frequency-domain far-field response was recorded for 17,000 FDTD time steps and is shown in Figure 6. Sampling for the GPOF method began at the 2000th step with $N = 200$ data points and a sam-

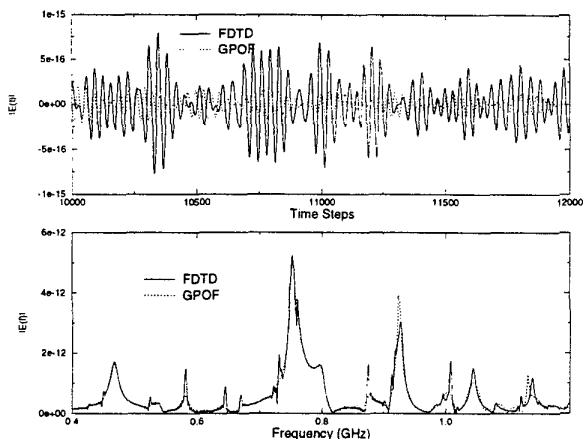


Figure 6. A comparison between FDTD and GPOF far-field time responses from a cavity geometry in the time domain (upper), and frequency domain (domain).

pling interval of 10 was used. The guidelines suggested by Table I and Figure 1 were followed. However, since this sequence was more rapidly oscillating in time, the competing demands of increasing d to get a smaller condition number, and decreasing d to capture the oscillations to strive for accuracy is severe. The criteria for singular value elimination σ was reduced to 8×10^{-2} to give more tolerance for stability. As indicated previously, a larger σ helps for stability but also degrades accuracy and reduces M . Only 15 exponential terms were obtained from the GPOF algorithm. The SNR is only 7 dB, indicating poor accuracy. However this was the only stable solution of more than 20 attempts with different combinations of input parameters. Furthermore, the sensitivity of stability and accuracy to the input parameters was very high for this problem. The discrepancy between the reconstructed GPOF time history and the FDTD simulation is significant as shown in Figure 6.

V. CONCLUSIONS

The application of GPOF in FDTD modeling of EMI antenna geometry is promising due to its relatively low-Q. Specifying the input parameters n_i , σ , N and L for the open region problem is relatively straightforward. Achieving an accurate extrapolation is not particularly sensitive to the inputs. A significant amount of computation time can be saved by applying GPOF to these open region problems. In the shielding enclosure geometry, however, the advantage of the GPOF method varies on case by case basis. Guidelines can help to increase the possibility of reaching stable and acceptable solution, but only to a limited degree. Difficulties in balancing a stable solution with acceptable accuracy can arise in high-Q resonant structures with closely spaced frequency.

REFERENCES

[1] Z. Bi, Y. Shen, K. L. Wu, "Fast finite-difference time domain analysis of resonators using digital filtering and

spectrum estimation technique," *IEEE Transactions on Microwave Theory and Technology*, vol. 40 pp. 1611-1619, Aug. 1992.

[2] W. Kuempel, I. Wolff, "Digital signal processing of time-domain field simulation results using the system identification method," *IEEE MTT-S Digest*, pp. 793-796, 1992.

[3] W. L. Ko, R. Mittra, "A combination of FD-TD and Prony's methods for analyzing microwave integrated circuits," *IEEE Transactions on Microwave Theory and Techniques*, vol. 39, pp 2176-2181, Dec. 1991.

[4] T. K. Sarkar, J. N. Nebat, D. D. Weiner, and V. K. Jain, "Suboptimal approximation identification of transient waveforms from electromagnetic systems by pencil-of-function method," *IEEE Transactions on Antennas and Propagation*, AP-37, pp. 229-234, Feb. 1989.

[5] J. Chen, C. Wu, T. K. Y. Lo, "Using linear and nonlinear predictors to improve the computational efficiency of the FDTD algorithm," *IEEE Transactions on Microwave Theory and Techniques*, vol. 42, pp. 1992-1997, Oct. 1994.

[6] R. Kumaresan, D.E. Tufts, "Estimating the parameters of exponentially damped sinusoids and pole-zero modeling in noise," *IEEE Transactions on Acoustics, Speeches, and Signal Processing*, vol. ASSP-30, No. 6, pp. 833-840, Dec. 1982.

[7] T. K. Sarkar and O. Pereira, "Using the matrix pencil method to estimate the parameters of a sum of complex exponentials," *IEEE Antenna and Propagation Magazine*, vol.3, pp. 48-55, Feb. 1995.

[8] Y. Hua, T. K. Sarkar, "Generalized Pencil-of-Function Method for extracting poles of an EM system from its transient response," *IEEE Antenna and Propagation Magazine*, vol. 37, pp. 229-234, Feb. 1989.

[9] D.G.Dudley, "Parameter modeling of transient electromagnetic systems," *Radio Sci.*, vol. 14, pp. 38-396, May-June 1979.

[10] J.N. Franklin, "Well-posed stochastic extension of ill-posed linear problems," *J. Math. Anal. Appl.*, vol. 31, pp. 682-716, Aug. 1970.

[11] R. W. Kulp, "An optimum sampling procedure for use with the prony method," *IEEE Transactions on Electromagnetic Compatibility*, vol. EMC-23, pp. 67-71, May 1981.

[12] R. S. Adve, T. K. Sarkar, O. M. C. Pereria-Filho, S. M. Rao, "Extrapolating of time-domain responses from three-dimensional conducting objects utilizing the matrix pencil technique," *IEEE Transactions on Antennas and Propagation*, vol. 45, pp 147-155, Jan. 1997.

[13] F. B. Hildebrand, *Introduction to Numerical Analysis*. New York, NY: Dover Publications, Inc., 1987.

[14] A. Taflov, *Computational Electrodynamics: The Finite-Difference Time-Domain Method*. Norwood, MA: Artech House, 1995.

[15] M. Li, Y. Ji, S.Radu, J. Nuebel, W. Cui, J. L. Drewniak "EMI from aperture at enclosure cavity mode resonance," *IEEE Electromagnetic Compatibility Symposium Proceedings*, pp 183-187, Austin, TX, 1997.

[16] W. Cui, H. Shi, X. Luo, F. Sha, J.L. Drewniak "Lumped-element sections for modeling coupling between high-speed digital and I/O line," *IEEE Electromagnetic Compatibility Symposium Proceedings*, pp 260-271, Austin, TX, 1997.